Efficient Analysis of Multilayer Microstrip Problems by Modified Fast Directional Multilevel Algorithm

Hua Chen [1, 2]

[1]Faculty of Science, Kunming University of Science and Technology, Kunming, 650500, China
93056460@qq.com

[2] Key Laboratory of Unconventional Metallurgy, Ministry of Education, Kunming University of Science and Technology, Kunming 650093, China

Abstract **─** Fast directional multilevel algorithm (FDMA) combined with quad-tree structure is presented for analyzing multilayer microstrip problems. This method is successfully applied to analyze scattering in free space and it is extended to solve multilayer mircrostrip problems in this paper. The quad-tree structure is employed for the layer containing the microstrip patch, and then the defined of far field for every observed group is modified. There is only Kernel evaluation in low rank representation so that the surface-wave is extracted for the far-field Green's functions expansion when the dielectric substrate is thick or relative permittivity is large. The memory requirement and the CPU time per iteration of the multilayer microstrip structure is presented, which show the accuracy and efficiency of this method.

Index Terms - Modified fast directional multilevel algorithm, multilayer microstrip structures, S-parameters, and transmission coefficient.

I. INTRODUCTION

The method of moments (MoM) [1, 2] is preferred in the analysis of microstrip structures, such as mircrostrip antennas, microwave integrated circuits, and microstrip interconnects. The first kind is the so-called spectral domain MoM [3], which is time-consuming evaluation of doubly infinite integrals for integrands are highly oscillatory and decay slowly. The second kind is the spatial domain MoM, which is proposed by Michalski and Hsu in [4] for scattering by microstrip patch antennas in a multilayered medium. However, for large-scaled complex microstrip structures, it is impractical to solve resultant matrix equation because it has a memory requirement of O (N^2) and computational complexity is proportional to O (N^3). Many fast algorithms are developed to simulate large-scale microstrip problems, including frequency domain method [5-14] and spectral domain method [15-17]. The frequency domain method is more popular than spectral domain method because of escaping of Sommerfeld integral.

The frequency domain method includes the adaptive integral method (AIM) [5], the fast multipole algorithm (FMA) [6-8] and the multilevel matrix decomposition algorithm (MLMDA) [9], etc. These methods are successfully employed to analyze microstrip problems in conjunction with the discrete complex image method (DCIM) [10-11]. To be noticed, though the FMA is successfully applied to the microstrip problems, the procession is always difficult because of its dependence on the Green's function. At the beginning, FMA is tried to combine with DCIM to solve the static and two-dimensional problems [6]. Unfortunately, it will be lack of accuracy when the frequency is high. Though, FMA is employed in [7] for full wave analysis, the implementation is very complicated because the surface-wave poles are extracted in DCIM. The FMA also has been applied to thin layer structures as the thin stratified medium fast multipole algorithm [12], which is adaptive to thin-stratified media.

The fast directional multilevel algorithm is originally applied in the analysis of scattering problem of free space [13]. The method is Kernel independent and the Green's function is expanded by low rank representation, which is demonstrated efficiently in [13-14]. In this paper, the method is successfully applied to deal with planar microstrip structures in multilayered medium. There is only Kernel evaluation in low rank representation so that it is easily implemented in full wave analysis.

Submitted On: Nov. 29, 2012
Accepted On: Jan. 27, 2014

A quad-tree structure other than oct-tree structure is used for multilayered medium. However, the quad-tree structure is used for the layer, which contains the metallic patch. As a result, the definition of far field in our method has made some modifications. The DCIM is employed to efficiently evaluate the Sommerfeld integral and the surface wave contribution is considered for the far field of the Green's functions.

The interactions between the nearby groups are accounted for directly. For far apart groups, the interaction between the groups is accelerated by FDMA. The definition of high frequency regime and low frequency regime is the same as in the free space [13-14], except that the high frequency regime or low frequency regime in the neighboring layer must be considered now. Numerical results are presented to demonstrate the efficiency of this method.

II. FORMULATION

In this paper, the analysis is based on the mixed potential integral equation (MPIE) [14]. The microstrips are divided into triangular elements and the current is expanded using planar Rao-Wilton-Glisson (RWG) basis functions [2]. Consider a multilayered medium shown in Fig. 1. The dielectric constant of the substrates are ε_{r1}, ε_{r2}, ε_{r3}, etc, corresponding to the thickness d_1, d_2, d_3, etc. The boundary condition associated with the tangential electric field on a perfectly conducting surface, we obtain,

$$\hat{n}\times\mathbf{E}^s(\mathbf{r}) = -\hat{n}\times\left[\mathbf{E}^i(\mathbf{r})+\mathbf{E}^r(\mathbf{r})\right], \quad on \quad S \tag{1}$$

where $\mathbf{E}^s$ refers to the scattered field excited by the current on the conducting surface of the antenna S. $\mathbf{E}^i$ denotes the incident electric field. The MPIE can be written as,

$$j\omega\mu_0\hat{n}\times\left[\mathbf{A}(\mathbf{r})+\frac{1}{k_0^2}\nabla\Phi(\mathbf{r})\right] = \hat{n}\times\left[\mathbf{E}^i(\mathbf{r})+\mathbf{E}^r(\mathbf{r})\right] \tag{2}$$

where

$$\mathbf{A}(\mathbf{r}) = \iint_S G_a(\mathbf{r},\mathbf{r}')\cdot\mathbf{J}(\mathbf{r}')dS', \tag{3}$$

$$\Phi(\mathbf{r}) = \iint_S G_q(\mathbf{r},\mathbf{r}')\nabla\cdot\mathbf{J}(\mathbf{r}')dS'. \tag{4}$$

The symbol G_a denotes Green's functions for the magnetic vector potential while G_q for the electric scalar potential. Both G_a and G_q can be obtained by an inverse Hankel transform of their spectral domain Sommerfeld integral [17],

$$G_{a,q} = \int_{-\infty}^{+\infty}\tilde{G}_{a,q}H_0^{(2)}(k_\rho\rho)k_\rho dk_\rho. \tag{5}$$

Both G_a and G_q are formed by three parts respectively,

$$G_a = G_{a0}+G_{a,ci}+G_{a,sw} \tag{6}$$

$$G_q = G_{q0}+G_{q,ci}+G_{q,sw}. \tag{7}$$

G_{a0} and G_{q0} represent the contribution from the quasi-dynamic images, which dominate in the near-field region,

$$G_{a0} = \frac{\mu_0}{4\pi}\left(\frac{e^{-jk_0r_0}}{r_0}-\frac{e^{-jk_0r_0'}}{r_0'}\right) \tag{8}$$

$$G_{q0} = \frac{1}{4\pi\varepsilon_0}\left(\frac{e^{-jk_0r_0}}{r_0}+K\frac{e^{-jk_0r_0''}}{r_0''}+\sum_{n=1}^{\infty}K^{n-1}(K^2-1)\frac{e^{-jk_0r_n}}{r_n}\right), \tag{9}$$

where $K=(1-\varepsilon_r)/(1+\varepsilon_r)$. $G_{a,ci}$ and $G_{q,ci}$ represent the contribution from the complex images, which dominates in the intermediate region. They can be obtained by applying DCIM and using Sommerfeld identity,

$$G_{a,ci} = \frac{\mu_0}{4\pi}\sum_{i=1}^{N}a_i\frac{e^{-jk_0r_i}}{r_i} \tag{10}$$

$$G_{q,ci} = \frac{1}{4\pi\varepsilon_0}\sum_{i=1}^{N}a_i'\frac{e^{-jk_0r_i'}}{r_i'}. \tag{11}$$

The third part stands for the contribution from the surface waves, which dominates in the far-field region,

$$G_{a,sw} = \frac{\mu_0}{4\pi}(-2\pi j)\mathrm{Res}_1H_0^{(2)}(k_{\rho p}\rho)k_{\rho p} \tag{12}$$

$$G_{q,sw} = \frac{1}{4\pi\varepsilon_0}(-2\pi j)\mathrm{Res}_2H_0^{(2)}(k_{\rho p}\rho)k_{\rho p}. \tag{13}$$

In the above equations, $r_n=\sqrt{\rho^2+(2nh)^2}$, h is the thickness of substrate. $r_i'=\sqrt{\rho^2-b_i^2}$ and $r_i''=\sqrt{\rho^2-b_i'^2}$, where a_i , a_i' , b_i and b_i' are complex coefficients obtained by Prony's method. Galerkin's method is applied, which results in a matrix equation,

$$\mathbf{ZI} = \mathbf{V}. \tag{14}$$

Using the fast directional multilevel algorithm, the matrix-vector product $\mathbf{ZI}$ can be written as,

$$\mathbf{ZI} = \mathbf{Z}_N\mathbf{I} + \mathbf{Z}_F\mathbf{I}$$

Here $\mathbf{Z}_N$ is the near part of $\mathbf{Z}$ and is computed directly. $\mathbf{Z}_F$ is the far part of $\mathbf{Z}$ and the computation of $\mathbf{Z}_F$ is accelerated by FDMA. Those elements in $\mathbf{Z}_F$ are not explicitly computed and stored.

III. FAST DIRECTIONAL MULTILEVEL ALGORITHM

The FDMA is originally developed in [14] for solving N-body or N-point problems. Then the algorithm is applied for electromagnetic scattering problem via combined field integral equation in [13]. After that, we leverage Calderlon identity for preconditioning FDMA to improve the convergence of EFIE [18-19]. Now, the FDMA is extended to solve multilayer microstrip problems.

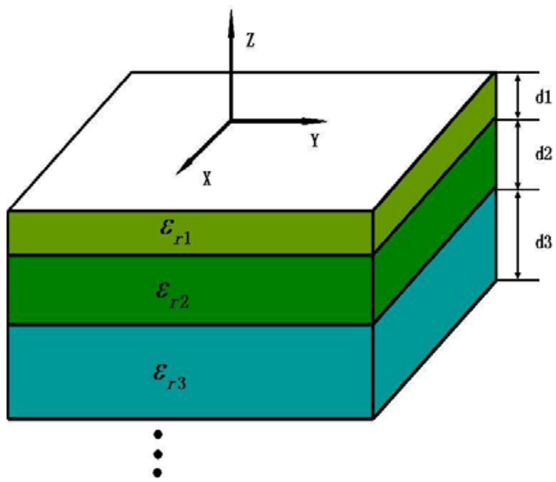

Fig. 1. The geometry of multilayered medium.

A. The construction of low rank representations

As in [13, 14, 17, 18], we need to construct low rank representations for Green's function. The most process of implementation for this part is the same except that the Green's function used here is described in equations (6) and (7). Quad-tree structure is employed here, which will be discussed in part B, therefore the random sampling is based on a square box,

$$G_a(\boldsymbol{r}_i,\boldsymbol{r}_j)\approx\sum_{p,q}G_a(\boldsymbol{r}_i,\boldsymbol{r}_p)d_{pq}G_a(\boldsymbol{r}_q,\boldsymbol{r}_j)\,. \quad (15)$$

We also need to construct the low rank representation for electric scalar potential G_q. Fortunately, the process is the same as above. It can be seen that the process of the construction in layered medium is almost the same as in free space described in [13]. Differently, We need to repeat the above process twice for G_a and G_q respectively, corresponding to store two sets of locations $\{\boldsymbol{r}_p\}$, $\{\boldsymbol{r}_q\}$ and the matrix $\mathbf{D}$ for every layer. The detailed implementation of FDMA using MPIE formulation can refer to [13, 14, 17, 18].

B. The quad-tree structure for layered medium

The oct-tree structure is usually used for three dimension structures with layered medium. Therefore, the oct-tree is originally adopted for the multilayer microstrip problem, but it is not memory efficient because of the three dimension sampling in part A. In this paper, quad-tree structure other than oct-tree is applied for multilayered medium and we make some modification when quad-tree structure is adopted. Take two-layered medium for example, and assume that metallic patch is contained in two-layered medium.

We first enclose all the patches of the first layer in a small square box, then the box is subdivided into small boxes until the smallest box at the lowest level. The boxes are organized into a quad-tree structure with the smallest boxes at the bottom of the inverted tree, and the largest box at the root of the inverted tree. The same operation is done for the second layer. We can get the final quad-tree structure for two layers shown in Fig. 2 (a) - (b). Figure 2 (a) stands for the grouping method in the low frequency regime, and the group size is smaller than one wavelength. Figure 2 (b) stands for the group size, is larger than one wavelength in the high frequency regime.

Assuming that the blue box Y in the first level is the observed box, and the corresponding box of Y in the second layer is also in blue color. All the boxes of two layers in red color are defined as the near field area of box Y while the boxes in yellow color are defined as the far field area. In other words, the boxes in yellow color of the two layers are all the far field interaction group of observed box Y. It is because that the thickness of the substrate is always thin, therefore, we can define the far field boxes of Y are all the yellow boxes in both layers.

IV. NUMERICAL RESULTS

In this section, a number of numerical examples are presented to demonstrate the efficiency of the FDMA for solving linear systems arising from the discretization of MPIE for analyzing microstrip structures. In the implementation of the FDMA, the restarted version of GMRES algorithm [20] is used as the iterative method. All experiments are performed Core-2 8400 with 3 GHz CPU and 4 GB RAM in double precision. The iteration process is terminated when the normalized backward error is reduced by 10^{-3} for all examples.

The first example concerns the *S*-parameters from a four-section low-pass filter [21]. The geometry is depicted in Fig. 3 (a), where ε_r= 10.8 and the substrate thickness is d = 0.0254 *mm*. The width of the patch are L_1=10.12 *mm*, L_2=6.12 *mm*, L_3=2.8 *mm*, L_4=1.3 *mm*, L_5=9.8 *mm*, L_6=3.5 *mm*, with W_s=1 *mm*, W=W_c= 0.3 *mm*, W_5 = 0.2 *mm*, W_6 = 4 *mm*, W_f = 0.57 *mm*, G = 0.2 *mm*, L_c = 1.78 *mm*, and L_f = 15 *mm*. The unit voltage source is applied and the S-parameters of this low-pass filter are shown in Fig. 3 (b). One level FDMA is used here and the finest group size is no larger than 0.05 λ at the smallest frequency. The results from FEKO [22] are also given in Fig. 3 (b) for comparison. Our results are in well agreement with the results from FEKO.

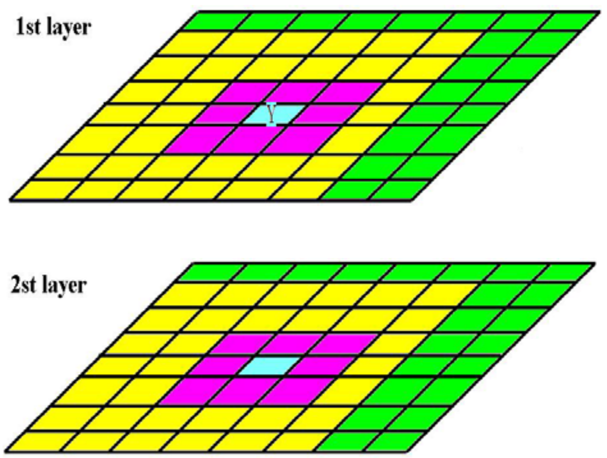

(a)

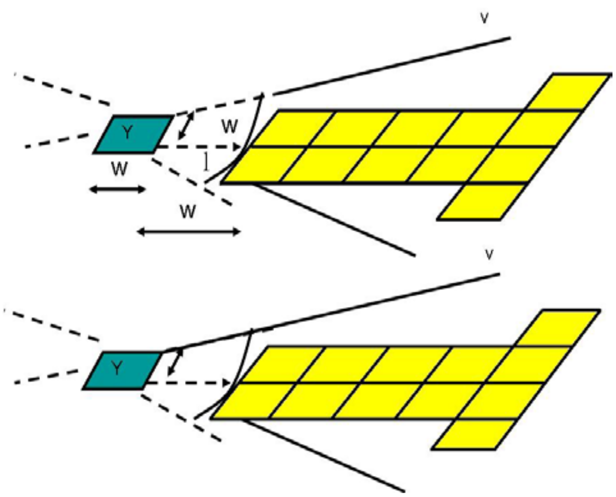

(b)

Fig. 2. (a) The grouping method for two layer-media in the low frequency regime and (b) the grouping method for two layer-media in the high frequency regime.

It can be observed that the results of the S-parameter are in well agreement below 4 GHz and 8 GHz to 10 GHz. Though, the agreement with the FEKO between 4 GHz to 8 GHz is not good, it can be satisfied with the engineering requirement because the S-parameters are all below 40 dB. It can be concluded that the FDMA is stable even at low frequency regime.

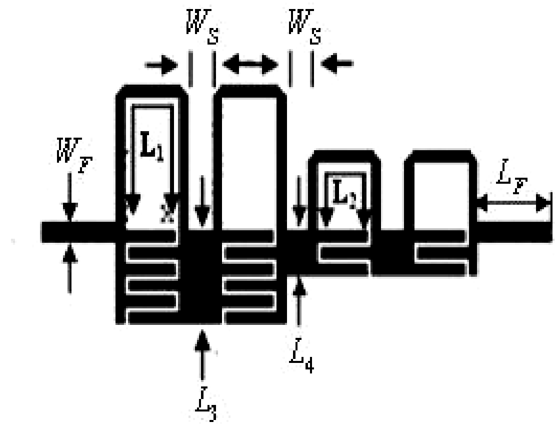

(a)

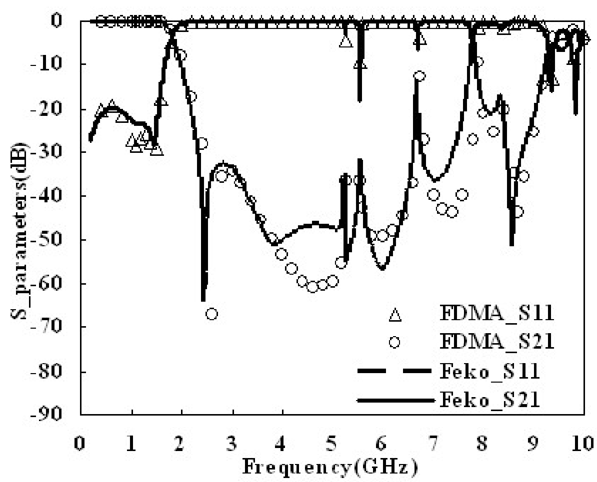

(b)

Fig. 3. (a) The configuration of four-section low-pass filter and (b) S-parameters of the four-section low-pass filter.

The following example is a quasi-periodic structure, which is analyzed as two layers microstrip structures with relative permittivity ε_r = 3.38. FDTD or FEM is often used for the simulation of periodic structure. Some new methods also come forth to deal with such special problem [23-24]. Though, different from common microstrip structure, the process of FDMA for periodic structure is the same as microstrip structure.

The proposed quasi-periodic structure with seven periods is shown in Fig. 4 (a)-(c). In our simulation, the unit voltage source is applied, with f_0 = 3GHz. We applied quad-tree in the first level for mircostrip line and in the second level for metal patch. We use three levels FDMA, and the results of *S*-parameters in Figs. 5 and 6 agree well with the results simulated by Ansoft designer.

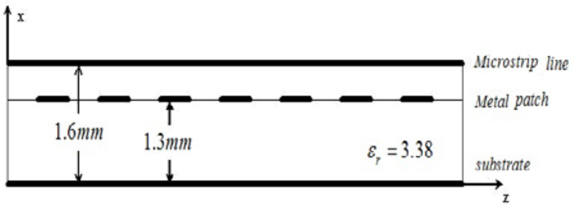

(a)

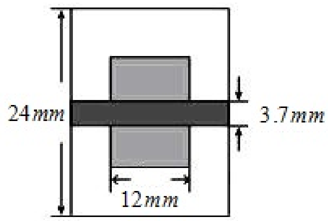

(b)

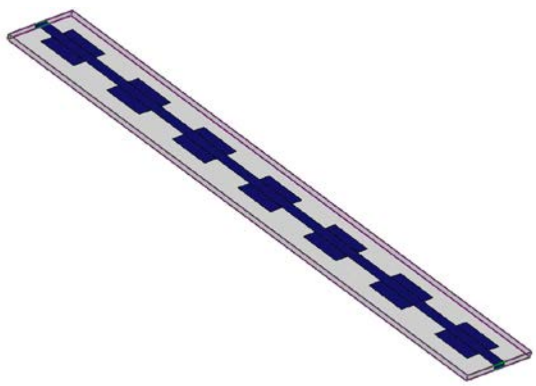

(c)

Fig. 4. (a) The configuration of a microstrip EBG structure, (b) proposed microstrip EBG structure, and (c) top view of a cell of the proposed microstrip EBG structure.

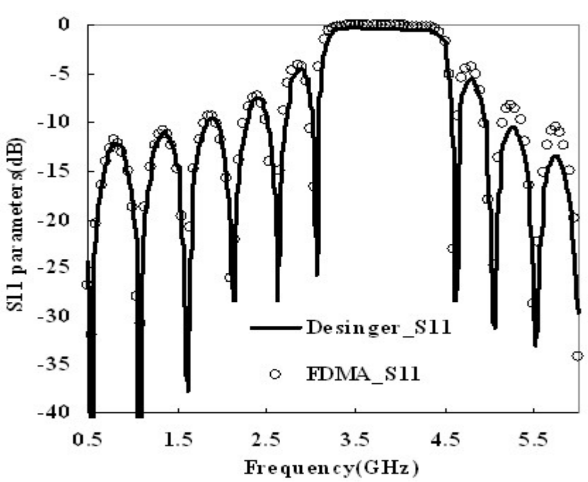

Fig. 5. S11 parameter of the EBG structure.

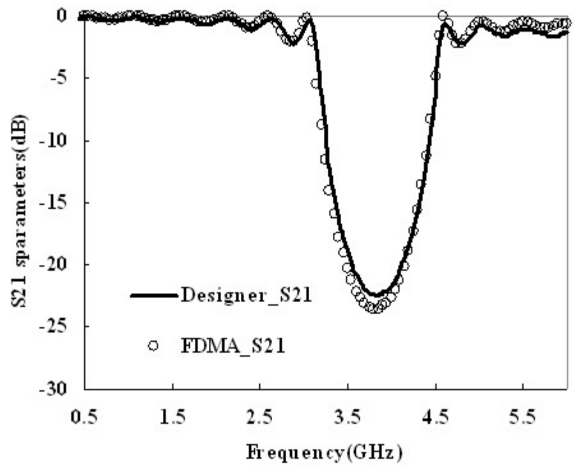

Fig. 6. S21 parameter of the EBG structure.

The next structure is a finite planar frequency selective surface (FSS). The transmission coefficient is defined as,

$$T = \left|-E^{ia} + E^{s}\right|^2 \Big/ \left|E^{ia}\right|^2 \qquad (16)$$

where E^{ia} denotes the quantities relative to the incident field and E^{s} is the far field at the transmission direction or the reflection direction. Our theoretic foundation is that the reflection coefficient of the metallic plate is 1 while its transmission coefficient is 0. Since the metallic plate is special form FSS. It implies that we can calculate E^{ia} using the far field of the metallic plate. It is obvious to obtain that $E^{ia} = -E^{s}_{metallic\ plate}$ at the transmission direction. $E^{s}_{metallic\ plate}$ denotes the far field of the metallic plate under the same incident plane wave. Then the transmission coefficient of general finite FSS can be calculated using,

$$T = \left|-E^{s}_{metallic\ plate} + E^{s}\right|^2 \Big/ \left|E^{s}_{metallic\ plate}\right|^2 . \qquad (17)$$

The transmission of the octagonal loop FSS embedded in a three-layered medium is investigated. The FSS array consists of 20×20 octagonal loop elements with number of unknowns 25600 as shown in Fig. 7. The dielectric constant of the substrates are ε_{r1} = 3.0, ε_{r2} = 1.0006, and ε_{r3} = 3.0 and the corresponding thickness of the substrates are 0.18 *mm*, 10.0 *mm*, and 0.18 *mm*, respectively. The outer radius of the element is 3.5 *mm* and the inner radius is 3 *mm*. The dimensions of the unit are T_x = 8 *mm*, T_y = 8 *mm*. The incident wave is TE polarization wave with $\theta^i = 30^\circ, \phi^i = 0^\circ$ and the skew angle is 60^o. The patch of octagonal loop FSS is in the third layer, as a result, we just employed the quad-tree in the third level. The three-level FDMA is used here. As shown in Fig. 8, the transmission coefficients of the 20×20 octagonal loop FSS arrays are plotted. It can be observed that the transmission coefficient of the finite FSS simulated by our method has a good agreement with the characteristic of the infinite FSS simulated by Ansoft designer.

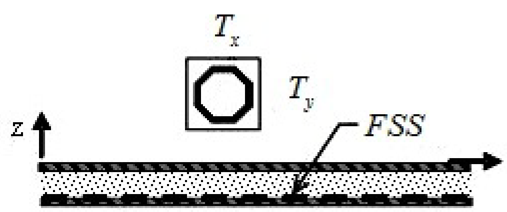

Fig. 7. The configuration of the octagonal loop FSS.

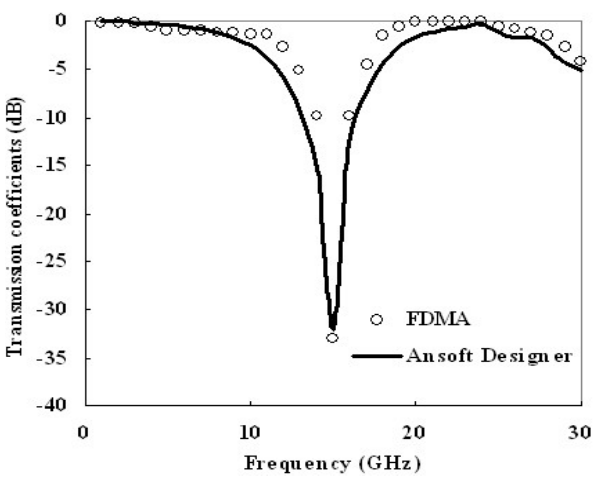

Fig. 8. The transmission loss curves versus frequency by the octagonal loop FSS arrays.

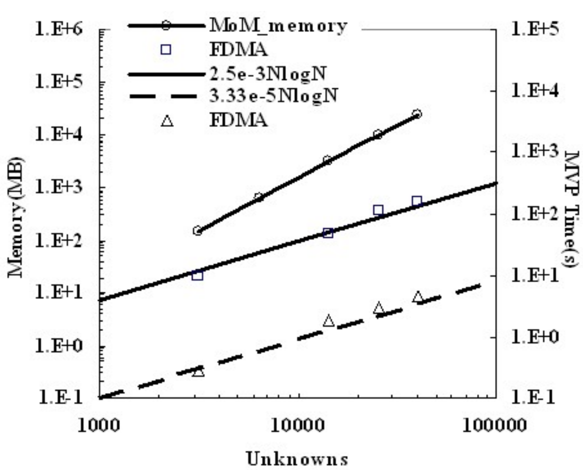

Fig. 9. The Complexity of FDMA for memory requirement and MVP time per iteration.

In this part, a series FSS array which consists of 8×8, 15×15, 20×20, and 25×25 octagonal loop elements are considered. The dielectric constant and the configuration of the octagonal loop FSS are the same as above. Assuming the incident angles of plan wave are θ^i = 30°, ϕ^i = 0° at 15 GHz. The matrix vector product (MVP) time per iteration and the memory requirement versus the number of unknowns are plotted in Fig. 9. It is can be observed that the CPU time per iteration and the memory requirement are all scaled as O (N Log N).

VI. CONCLUSION

In this paper, the fast directional multilevel algorithm is first applied for analyzing multilayer microstrip problems. The EBG structure and the finite FSS arrays are considered as multilayer microstrip structure, while the corresponding S-parameters and transmission coefficient are computed. The new method is easily implemented because it is Kernel independent. With the aid of DCIM, the MPIE is discretized in the spatial domain. The efficiency of this method is demonstrated by numerical results.

ACKNOWLEDGMENT

The author would like to thank Dr. Jiang Zhaoneng for providing useful discussions and Prof. R. S. Chen for his useful instruction. Thank the support of the International S&T Cooperation Program of China (No.2012DFA70570), the Yunnan Provincial International Cooperative Program (No. 2011IA004), Yunnan Provincial Foundation Program (No. 2013FZ016), the National Technology Research and Development Program of China (No. 2013AA064003), National Science Foundation of China (No. 51304097).

REFERENCES

[1] R. F. Harrington, *Field Computation by Moment Methods*, Malabar, Fla.: R. E. Krieger, 1968.

[2] S. M. Rao, D. R. Wilton, and A. W. Glisson, “Electromagnetic scattering by surfaces of arbitrary shape,” *IEEE Trans. Antennas Propag*., vol. 30, no. 3, pp. 409-418, 1982.

[3] E. H. Newman and D. Forrai, “Scattering from a microstrip patch,” *IEEE Trans. Antennas Propagat.*, vol. 35, pp. 245-251, March 1987.

[4] K. A. Michalski and C. G. Hsu, “RCS computation of coax-loaded microstrip patch antennas of arbitrary shape,” *Electromag.*, vol. 14, Jan. ~ Mar., pp. 33-62,1994.

[5] F. Ling, C. F. Wang, and J. M. Jin, “An efficient algorithm for analyzing large-scale microstrip

structures using adaptive integral method combined with discrete complex image method," in *IEEE APS Int. Symp. Dig*., vol. 3, pp. 1778-1781, 1998.

[6] L. Gurel and M. I. Aksun, "Electromagnetic scattering solution of conducting strips in layered media using the fast multipole method," *IEEE Microwave Guided Wave Lett.*, vol. 6, pp. 277-279, Aug. 1996.

[7] P. A. Macdonald and T. Itoh, "Fast simulation of microstrip structures using the fast multipole method," *Int. J. Numer. Modeling: Electron. Networks, Devices, Fields*, vol. 9, pp. 345-357, 1996.

[8] F. Ling, J. M. Song, and J. M. Jin, "Multilevel fast multipole algorithm for analysis of large-scale microstrip structures," *IEEE Microwave Guided Wave Lett.*, vol. 9, pp. 508-510, Dec. 1999.

[9] J. Parron, J. M. Rius, and J. R. Mosig, "Application of the multilevel matrix decomposition algorithm to the frequency analysis of large microstrip antenna arrays," *IEEE Trans. Magn*., vol. 38, no. 2, pp. 721-724, Mar. 2002.

[10] D. G. Fang, J. J. Yang, and G. Y. Delisle, "Discrete image theory for horizontal electric dipoles in a multilayered medium," *Proc. IEEE, Pt. H*, vol. 135, pp. 297-303, Oct. 1988.

[11] Y. L. Chow, J. J. Yang, D. G. Fang, and G. E. Howard, "A closed-form spatial Green's function for the thick microstrip substrate," *IEEE Trans. Microwave Theory Tech.*, vol. 39, pp. 588-592, Mar. 1991.

[12] J. S. Zhao, W. C. Chew, C. C. Lu, E. Michielssen, and J. M. Song, "Thin-stratified medium fast-multipole algorithm for solving microstrip structures," *IEEE Trans. Microwave Theory Tech*., vol. 46, pp. 395-403, Apr. 1998

[13] H. Chen, K. W. Leung, and E. N. Yung, "Fast directional multilevel algorithms for analyzing wave scattering," *IEEE Trans. Antennas Propag.*, vol. 59, no. 7, July, pp. 962-974, 2011.

[14] B. Engquist and L. Ying, "Fast directional multilevel algorithms for oscillatory kernels," *SIAM Journal on Scientific Computing*, vol. 29, no. 4, pp. 1710-1737, 2007.

[15] T. Vaupel, "A fast spectral domain solver for the characterization of large microwave structures in multilayered environments," *Applied Computational Electromagnetics Society* (ACES) *Journal*, vol. 24, no. 5, pp. 493-503, October 2009.

[16] K. A. Michalski and J. R. Mosig. "Multilayered media Green's functions in integral equation formulations," *IEEE Transaction on Antennas and Propag*., vol. 3, pp. 508-519, 1997.

[17] K. Michalski and D. Zheng "Electromagnetie scattering and radiation by surfaces of arbitrary surfaces of arbitrary shape in layered media, Part I: Theory," *IEEE Trans. Antennas Propag*., vol. 38, no. 3, pp. 335-344, Aug. 1990.

[18] H. Chen, J. Zhu, R. S. Chen, and Z. H. Fan, "Fast direction multilevel algorithm combined with Calderon multiplicative preconditioner for stable electromagnetic scattering analysis," *Microwave Opt. Technol. Lett.*, vol. 52, no. 9, pp. 1963-1969, 2010.

[19] H. Chen, J. Zhu, R. S. Chen, and Z. H. Fan, "Calderon multiplicative preconditioner for acceleration of fast direction multilevel algorithm for scattering problem," *Proceedings ICMMT*, Chengdu, P. R. China, 8-11 May, 2010.

[20] Y. Saad, *Iterative Methods for Sparse Linear System*, PWS Publishing Company, 1996.

[21] W. H. Tu and K. Chang, "Compact microstrip low-pass filter with sharp rejection," *IEEE Trans. Microw. Wireless Compon. Lett.*, vol. 15, no. 6, pp. 404-407, June 2006.

[22] U. Jakobus, M. Schoeman, J. Tonder, D. Ludick, and W. Burger, "Selection of new features in the electromagnetic solution kernel of FEKO suite 6.0," *27th Annual Review of Progress in Applied Computational Electromagnetics (ACES)*, pp. 308-313, Williamsburg, Virginia, March 2011.

[23] F. Hu, J. Song, and T. Kamgaing, "IE analysis of scattering from multilayered doubly periodic array of 3-D PEC objects using equivalence principle and connection scheme," *27th Annual Review of Progress in Applied Computational Electromagnetics (ACES)*, pp. 482-487, Williamsburg, Virginia, March 2011.

[24] E. A. Hajlaoui, H. Trabelsi, A. Gharsallah, and H. Baudrand, "Analysis of photonic band gap using multilayer contribution of wave concept iterative process MLC-WCIP," *Applied Computational Electromagnetics Society (ACES) Journal*, vol. 24, no. 3, pp. 352-357, June 2009.

Hua Chen was born in Anhui Province, China. She received her Ph.D. degree in Nanjing University of Science and Technology (NJUST), She is currently working in Kunming University of Science and Technology(KMUST), at Kunming, China. Her current research interests include computational electromagnetics, antennas and electromagnetic scattering and propagation, electromagnetic modeling of microwave integrated circuits.